STU
SLOVAK UNIVERSITY OF TECHNOLOGY IN BRATISLAVA

Journal of Electrical Engineering, Vol. 77, No. 4, 2026, pp. 412-418
https://reference-global.com/journal/JEE

Degradation of Mordant Blue 9 by BDD/TiO_2 photoelectrode using 3D printed photoreactor

Miroslav Behul[1], Marián Marton[1], Pavol Michniak[1], Jaroslav Bruncko[2], Marian Vojs[1]

This work investigates boron-doped diamond (BDD) / TiO_2 heterostructure photoelectrodes for the degradation of the organic dye Mordant Blue 9. The combination of BDD and TiO_2 enables enhanced photoelectrocatalytic activity under UV irradiation. The electrodes were characterized using scanning electron microscopy and Raman spectroscopy. Electrochemical behavior was studied using linear sweep voltammetry under UV illumination. The degradation efficiency was evaluated with and without applied bias voltage. Results demonstrate successful degradation of Mordant Blue 9 and a significant improvement in degradation rate when both UV irradiation and external potential are applied. The study confirms the suitability of BDD/TiO_2 structures for advanced water treatment applications.

Keywords: boron-doped diamond, TiO_2, photoelectrochemistry, water treatment, dye degradation

1 Introduction

Water contamination by organic dyes represents a serious environmental problem due to their toxicity, persistence, and resistance to conventional treatment methods. Advanced oxidation processes, particularly photoelectrocatalysis, have gained attention as effective methods for degrading such pollutants. In addition to dye contaminants, many emerging micropollutants exhibit high chemical stability and poor biodegradability, which limits the efficiency of conventional biological and physicochemical treatment approaches [1-3]. Boron-doped diamond (BDD) is a p-type semiconductor material with a wide electrochemical window, high chemical stability, and excellent charge transport properties, making it suitable for electrochemical and photoelectrochemical applications [4]. The compact diamond structure renders the n-type doping process challenging. Consequently, various materials, including ZnO and TiO_2 are employed to establish heterostructure p-n junctions with BDD [5, 6].

Titanium dioxide (TiO_2) is a well-known n-type semiconductor photocatalyst characterized by strong oxidizing ability, chemical stability, and efficient photogeneration of electron-hole pairs under UV irradiation [7]. The integration of p-type BDD with n-type TiO_2 leads to the formation of a p-n heterojunction, which promotes efficient separation of photogenerated charge carriers and suppresses electron-hole recombination, thereby enhancing the generation of reactive oxygen species and improving photoelectrocatalytic performance. The performance of the heterojunction can be further enhanced by structuring the BDD layer, which increases the local electric field intensity at the heterojunction interface [8]. Therefore, the development of BDD/TiO_2 heterostructure photoelectrodes represents a promising approach for enhancing the degradation efficiency of organic dyes such as Mordant Blue 9 under UV irradiation [9]. In this study, the performance of novel BDD/TiO_2 heterostructure photoelectrodes with nanostructured interface and anatase TiO_2 deposited by pulsed laser deposition was investigated for the degradation of Mordant blue 9 dye.

2 Experimental

2.1 Sample preparation

The deposition of BDD film was performed in a surface wave plasma system, the Linear Antenna Microwave Chemical Vapor Deposition Reactor (Scia cube 300, Germany). N-type (100) silicon substrates (1×1 cm^2) were used for BDD deposition. Prior to the BDD deposition, substrates were seeded in an ultrasonic bath in a suspension of 50 mg nanodiamond powder in 1 L of demineralized water for 40 min. The BDD film was deposited for 60 h in a CH_4/H_2 gas mixture with trimethylboron added. The concentration of CH_4 in H_2

[1] Institute of Electronics and Photonics, Faculty of Electrical Engineering and Information Technology, Slovak University of Technology in Bratislava, Ilkovičova 3, 841 04 Bratislava, Slovak Republic
[2] International Laser Centre, Slovak Centre of Scientific and Technical Information, Lamačská cesta 8A, 840 05 Bratislava, Slovak Republic
miroslav.behul@stuba.sk

https://doi.org/10.2478/jee-2026-0040, Print (till 2015) ISSN 1335-3632, On-line ISSN 1339-309X

was set to 2%, and the B/C ratio in the gas phase was set to 10 000 ppm to achieve semiconducting BDD. The power of the microwave generator was set to 6 kW. The substrate temperature was maintained at 700 °C during the growth process, and the process gas pressure was 25 Pa. The nano-structuring of BDD was achieved by dry etching in radiofrequency plasma generated in an oxygen atmosphere for a duration of 30 min at a pressure of 6 Pa and an applied power of 100 W [10]. The TiO_2 thin film was deposited on the nanostructured BDD layer by pulsed laser deposition using a sintered undoped TiO_2 target in an oxygen atmosphere at a pressure of 3 Pa [11]. The substrate temperature during the deposition was maintained at 400 °C. An excimer laser (ComPex Pro 205, 248 nm) was used as the ablation source. The laser pulse energy measured behind the 10×20 mm aperture was 206 mJ, corresponding to a laser fluence of approximately 2.8 $J \cdot cm^{-2}$. The pulse repetition rate was set to 50 Hz. For the preparation of the 100 nm thick TiO_2 layer, 7500 laser pulses were applied, corresponding to a deposition time of 2.5 min. The sample was analyzed by scanning electron microscopy (JEOL 7500f equipped with a cold cathode) and Raman spectroscopy with a He-Ne laser (633 nm).

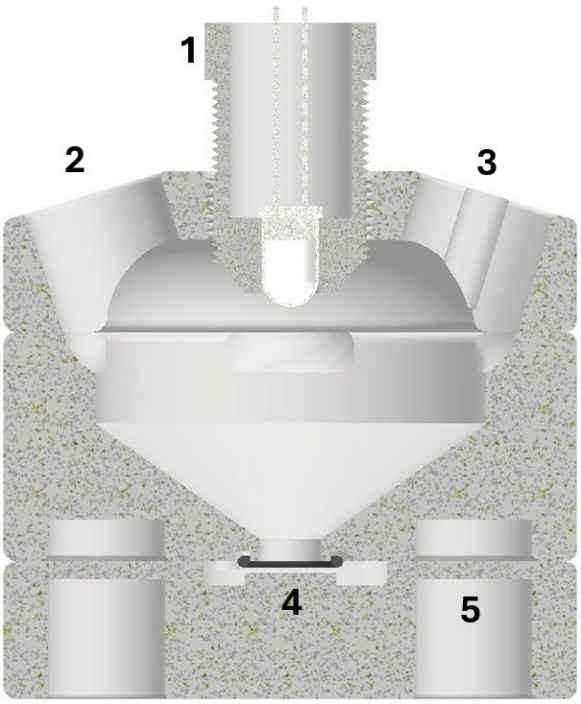

Fig. 1. Cross-sectional view of the 3D printed photoreactor consisting of 1) LED module, 2) Opening for reference electrode, 3) Opening for counter electrode, 4) Sample seating 5) Magnet based fitting

2.2 Photoelectrochemical measurements

The photoelectrochemical measurement was performed using Autolab PGSTAT 204 – Metrohm with linear sweep voltammetry at a scan rate of 5 mV/s in the range of −0.4 V to 0.8 V vs Ag/AgCl in 5 mL of 0.5 M Na_2SO_4 electrolyte. The photoelectrochemical degradation of 5 mL 20 µM Mordant Blue 9 prepared in 0.5 M Na_2SO_4 was performed using chronoamperometry at 0 V and 0.8 V vs Ag/AgCl. The three-electrode system with Pt serving as a counter electrode, Ag/AgCl serving as a reference electrode, and the BDD serving as the working electrode was used. UV LED with emission maxima at 365 nm and radiant power at the electrode surface of 1 mW/cm^2 was used for both linear sweep voltammetry (LSV) and degradation measurement.

2.3 3D printed photoreactor

The photoelectrochemical flow cell (PECell) was designed using Autodesk Inventor Professional 2025 and fabricated by stereolithography (SLA) 3D printing using a Prusa SL1S printer and an ABS-like photo-polymer resin (V2.0, ELEGOO Inc.) (Fig. 1). The UV exposure time for each 50 µm layer was optimized to 9 s. After printing, the parts were washed in isopropanol and post-cured under UV irradiation for 30 minutes.

The PECell consists of three parts that are joined by magnetic force, enabling fast assembly and disassembly. The bottom part contains a banana connector for the electrical connection and an opening for the working electrode (sample) with dimensions of 1×1 cm. The middle part contains a 5 mL electrolyte chamber and an O-ring seal that defines the circular active area of the working electrode with a diameter of 5.5 mm. The top part contains openings for the reference electrode, counter electrode, and an interchangeable LED module designed for 5 mm through-hole LEDs. The threaded mounting of the LED module enables precise adjustment of the distance between the LED and the working electrode. In addition, the modular design allows easy replacement of LED modules equipped with LEDs of different wavelengths.

3 Results and discussion

SEM analysis (Fig. 2) confirms the successful fabrication of nanostructured boron-doped diamond (BDD) film and sub-micro grain size of subsequently deposited TiO_2. The coexistence of both materials suggests the formation of a heterojunction, which plays a crucial role in the charge separation process [8].

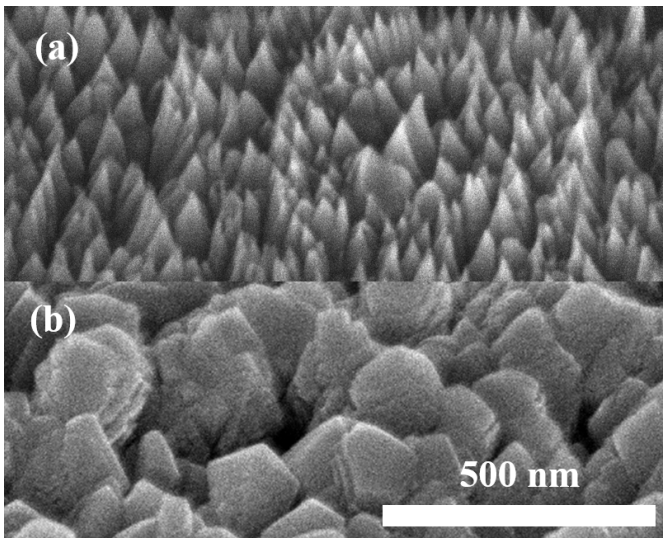

Fig. 2. SEM images of nanostructured BDD (a) and TiO_2-coated (b) electrode

Raman spectra (Fig. 3) show the characteristic diamond-related band (ZPC_D) at 1320 cm^{-1} confirming the formation of the BDD film. Broad bands observed near 1150 and 1450 cm^{-1} are associated with trans-polyacetylene (t-PA) species typically present in nanocrystalline diamond films [4]. Raman peaks assigned to TiO_2, particularly the anatase modes at 147 cm^{-1}, 398 cm^{-1}, and 618 cm^{-1}, further confirm the successful formation of the anatase phase of TiO_2 [8]. Due to the low doping level of BDD, the typical boron related maxima at approximately 500 and 1200 cm^{-1} are not present in the spectra. However, the red-shift of the ZPC_D maximum from its original position at 1332 cm^{-1} suggests the occurrence of a mild Fano effect, indicating the achievement of the metal-insulator transition threshold [12].

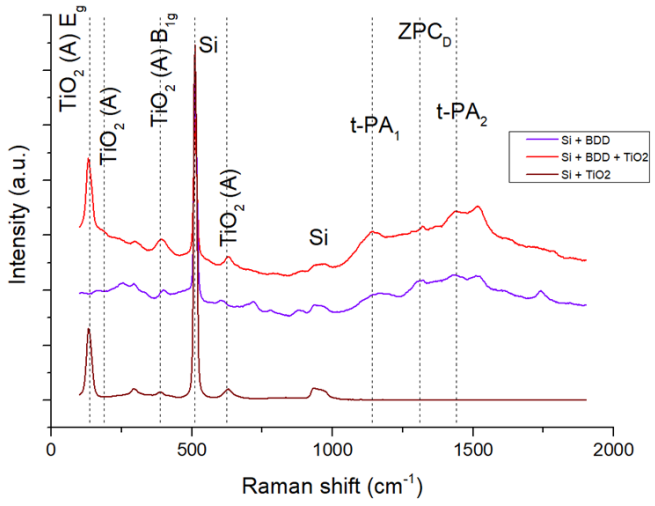

Fig. 3. Raman spectra of BDD and BDD/TiO_2 electrodes

LSV measurements of the BDD/TiO_2 photoelectrode under different LED intensities showed a significant increase in photocurrent with increasing illumination (Fig. 4). The sharp current rise near 0 V vs. Ag/AgCl confirms efficient photoinduced charge generation and separation in the TiO_2 layer, while the quasi-plateau region observed at higher potentials indicates saturation of charge carrier transport and electrochemical reactions.

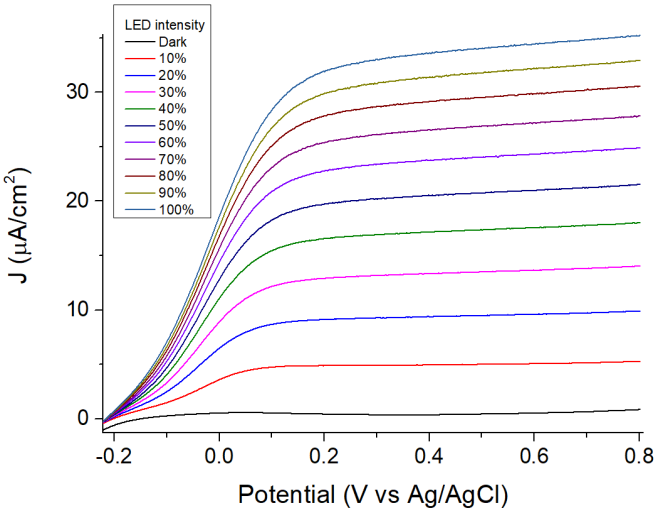

Fig. 4. LSV curves recorded under different intensity of UV irradiation

Figure 5 illustrates the evolution of the photocurrent density as a function of LED intensity at 0 V and at a bias potential of 0.8 V vs Ag/AgCl. The application of external anodic bias potential significantly enhanced the photocurrent and linearized the photoresponse across the investigated light intensity range. This improvement is attributed to the enhanced separation efficiency of photogenerated charge carriers within the hetero-structure [13]. However, the linear behavior of the curve is constrained at higher illumination levels, which generate more charge carriers, suggesting that the charge separation could be further improved by increasing the applied voltage.

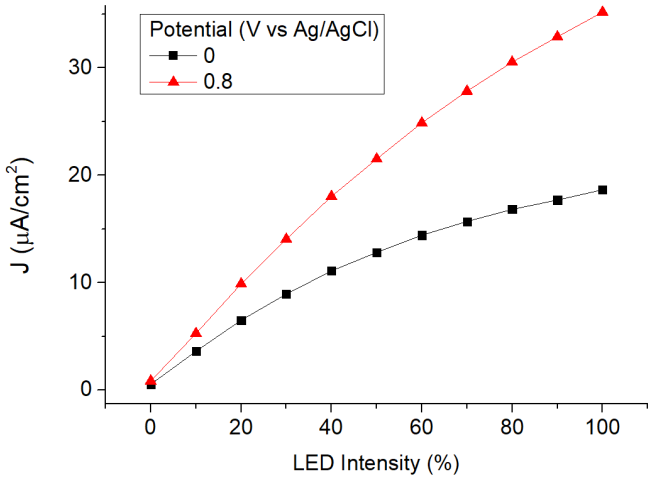

Fig. 5. Influence of irradiation intensity on the photo-current

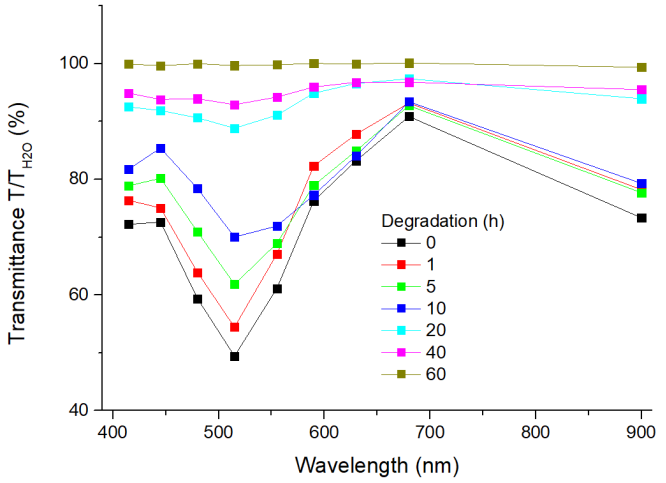

Fig. 7. Measured transmittance spectra evolution during degradation of MB9 at 0.8 V (vs. Ag/AgCl)

Figures 6 and 7 show the evolution of the mea-sured transmittance spectrum during the photo-electrochemical degradation of MB9 at 0 and 0.8 V vs. Ag/AgCl, measured by the photodiode field based photo-spectrometer. The measured transmittance minimum at 520 nm, maximum at 680 nm, and the overall shape of the spectrum correspond with the absorbance spectrum of MB9 [14]. Over the course of the degradation process, the entire spectrum steadily shifts toward 100% transmittance, visually demonstrating the successful purification of the solution across the visible light range. While the unbiased system at 0 V shows a gradual uniform progression towards transparency across all recorded wavelengths, requiring 60 hours, the 0.8 V bias potential induces a flattening of the transmission over the entire spectrum after 20 hours, confirming highly accelerated decolorization dynamics.

Figure 8 shows the time evolution of transmittance during degradation of MB9 with and without applied 0.8 V bias potential. Wavelength 515 nm corresponds to the characteristic absorbance maximum of Mordant Blue 9, associated with the azo chromophore structure of the dye molecule. In contrast, the absorption band observed at 590 nm is attributed to intermediate degradation products formed during the photoelectrocatalytic decomposition of MB9. The appearance and increase of this band during degradation indicates the formation of partially oxidized aromatic species and conjugated intermediates generated during the cleavage and subsequent transformation of the azo structure [14]. Applying bias voltage of 0.8 V significantly accelerated the degradation of Mordant Blue 9, a phenomenon attributable to the improved separation of photo-generated charge carriers and the suppression of

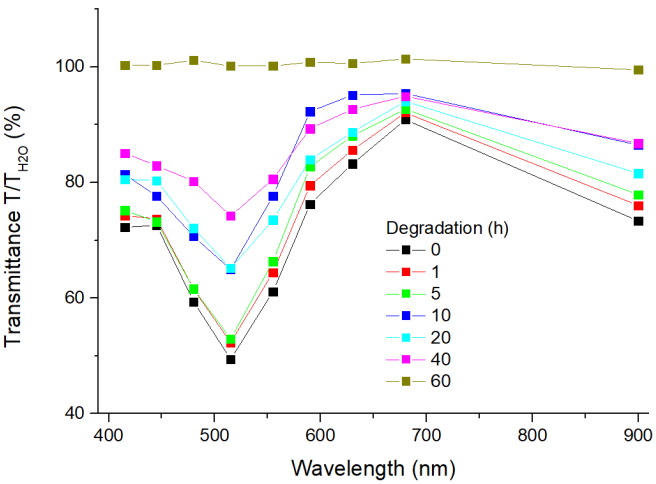

Fig. 6. Measured transmittance spectra evolution during degradation of MB9 at 0 V (vs. Ag/AgCl)

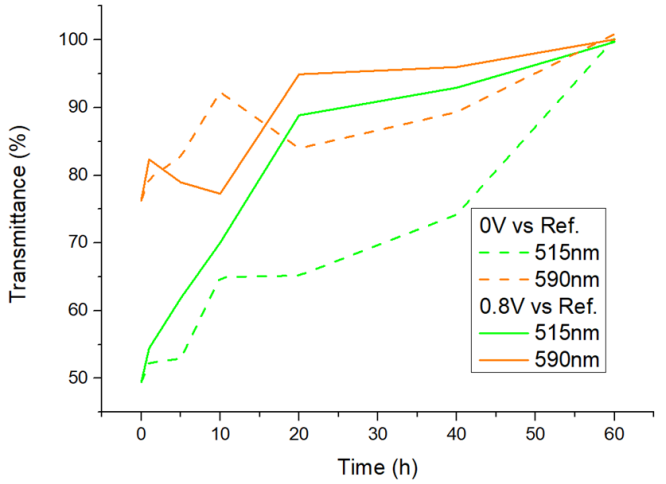

Fig. 8. Degradation of Mordant Blue 9 without and with applied bias voltage (Ref. is Ag/AgCl)

electron-hole recombination. This promoted the formation of reactive oxygen species, with hydroxyl radicals considered the primary contributor to the oxidative degradation of organic pollutants [15]. The observed synergistic effects highlight the advantage of the photoelectrocatalytic system in comparison to purely photocatalytic or electrochemical processes [16].

Photographic analysis (Fig. 9) visually confirms the enhanced degradation efficiency under combined UV irradiation and applied bias compared to UV irradiation alone. While both samples exhibit gradual decolorization over time, the solution treated at 0.8 V vs. Ag/AgCl becomes visibly transparent approximately 40 hours earlier, indicating a significantly faster decomposition of the dye molecules. The visual observations are in good agreement with the transmittance measurements presented in Figs. 6 and 7 and further demonstrate the beneficial effect of the external bias on the photoelectrochemical degradation process.

Table 1 summarizes selected studies performed under operating conditions comparable to those employed in this work. The degradation times reported in the literature are typically one or two orders shorter and the volumes of the dye-contained solutions are one or two orders higher. On the other side, photoelectrode surfaces are typically one or two orders larger and irradiation is one order higher. Therefore, the results obtained using BDD/TiO_2 photoelectrodes demonstrate the comparable capability of photocatalytic degradation of azo dye contaminated solutions with state-of-the-art results.

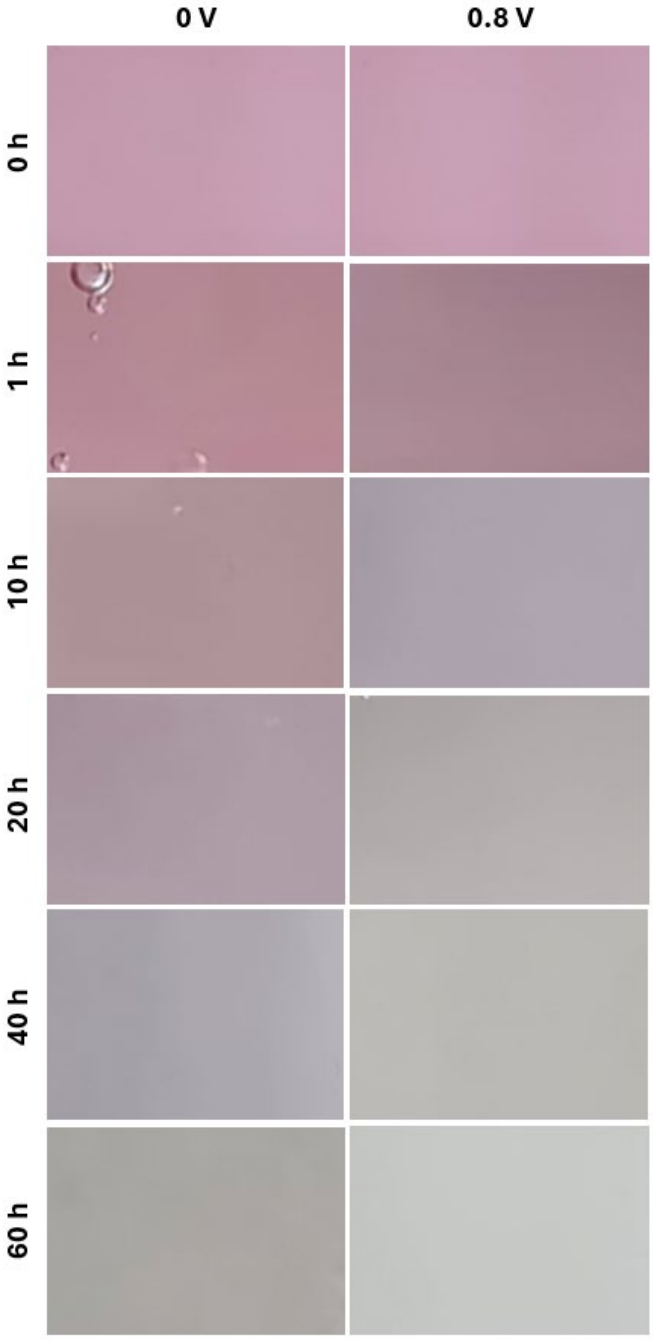

Fig. 9. Photographic comparison of dye degradation over time without applied potential and with applied bias potential of 0.8 V vs. Ag/AgCl

Table 1. Comparison of PEC experiments for removal of Azo dyes under similar operational conditions

Photoelectrode	Azo dye	Volume	UV Irradiance	Bias	Surface	Degradation time
BDD/TiO_2 *	20 µM MB9	5 mL	1 mW/cm^2	0 vs Ag/AgCl	0.2 cm^2	20h (65%), 60h (100%)
BDD/TiO_2 *	20 µM MB9	5 mL	1 mW/cm^2	0.8 vs Ag/AgCl	0.2 cm^2	20h (90%), 60h (100%)
Cu/S-TiO_2 [17]	156 µM BB9	125 mL	2 mW/cm^2	1 mA cm^{-2}	10 cm^2	1h (49%)
Porous TiO_2 [18]	47 µM RO9	30 mL	50 mW/cm^2	0.8 vs SCE	8 cm^2	0.5h (100%)
TiO_2 NTs [19]	31 µM BB	100 mL	10 mW/cm^2	0.6 vs Ag/AgCl	2 cm^2	1.75h (93.85%)
TiO_2/$SrTiO_3$ [19]	31 µM BB	100 mL	10 mW/cm^2	0.6 vs Ag/AgCl	2 cm^2	0.33h (100%)

*This work

4 Conclusion

BDD/TiO_2 photoelectrodes demonstrated ability of photoelectrocatalytic degradation of Mordant Blue 9 under UV irradiation. SEM and Raman analyses confirmed the successful fabrication of the BDD/TiO_2 heterostructure, while LSV measurements revealed enhanced photocurrent generation with increasing UV intensity, indicating efficient photogeneration and separation of charge carriers in the heterostructure. The application of an external anodic bias of 0.8 V vs. Ag/AgCl further increased the photocurrent response and improved the linearity of the photoresponse by promoting charge carrier separation and suppressing electron-hole recombination. Complete degradation of Mordant Blue 9 was achieved within 60 h even without an applied bias voltage, while the application of 0.8 V vs. Ag/AgCl significantly accelerated the degradation process. The developed 3D-printed photoreactor proved measurement repeatability and operational stability while providing simple handling, rapid assembly, and reproducible positioning of the electrodes and UV light source. The obtained results confirm the potential of BDD/TiO_2 heterostructures for advanced wastewater treatment applications.

Acknowledgement

This work was funded by the EU NextGenerationEU through the Recovery and Resilience Plan for Slovakia under the project No. 09I03–03-V04–00154.

References

[1] L. Zhang, X. Zhang, C. Wei, F. Wang, H. Wang, Z. Bian, "Interface engineering of Z-scheme α-Fe_2O_3/g-C_3N_4 photoanode: Simultaneous enhancement of charge separation and hole transportation for photoelectrocatalytic organic pollutant degradation", Chemical Engineering Journal, vol. 435, p. 134873, 2022.

[2] T. Mackuľak, E. Medvecká, A. Vojs Staňová, P. Brandeburová, R. Grabic, O. Golovko, M. Marton, I. Bodík, A. Medveďová, M. Gál, M. Planý, A. Kromka, V. Špalková, A. Škulcová, I. Horáková, M. Vojs, „Boron doped diamond electrode – The elimination of psychoactive drugs and resistant bacteria from wastewater", Vacuum, vol. 171, p. 108957, 2020.

[3] T. Mackuľak, M. Marton, M. Radičová, A. Vojs Staňová, R. Grabic, L. Bírošová, K. Nagyová, M. Vojs, I. Bodík, P. Brandeburová, M. Gál, „Monitoring of micropollutants and resistant bacteria in wastewater and their effective removal by boron doped diamond electrode", Monatshefte für Chemie - Chemical Monthly, vol. 148, no. 3, pp. 539–548, 2017.

[4] M. Vojs, M. Varga, O. Babchenko, M. Michniak, M. Marton, "Electrical characterization of diamond films deposited in nitrogen and oxygen containing gas mixture", Applied Surface Science, vol. 312, pp. 226–230, 2014.

[5] M. Marton, M. Mikolášek, J. Bruncko, I. Novotný, T. Ižák, M. Vojs, H. Kozak, M. Varga, A. Artemenko, A. Kromka, „Fabrication and Characterization of N-Type Zinc Oxide/P-Type Boron Doped Diamond Heterojunction", Journal of Electrical Engineering, vol. 66, no. 5, pp. 273–278, 2015.

[6] M. Behúl, M. Vojs, M. Marton, P. Michniak, M. Mikolášek, M. Kurniawan, H. L. Honig, D. V. Zyabkin, M. O. Ramirez, L. Spieß, D. Flock, A. Bund, M. Papula, R. Redhammer, „Nanostructured boron doped diamond enhancing the photoelectrochemical performance of TiO_2/BDD heterojunction anodes", Vacuum, vol. 171, p. 109006, 2020.

[7] U. Diebold, "The surface science of titanium dioxide", Surface Science Reports, vol. 48, no. 5-8, pp. 53-229, 2003.

[8] M. Behul, M. Vojs, M. Marton et al., "Nanoscale Engineering of Si/BDD/TiO_2 heterostructure interfaces to enhance photoelectrochemical performance", Applied Surface Science Advances, vol. 27, p. 100757, 2025.

[9] M. R. Hoffmann, S. T. Martin, W. Choi, D. W. Bahnemann, "Environmental Applications of Semiconductor Photocatalysis", Chemical Reviews, vol. 95, no. 1, pp. 69–96, 1995.

[10] M. Marton, M. Ritomsky, P. Michniak, M. Behul, V. Rehacek, R. Redhammer, A. Vincze, M. Papula, M. Vojs, „Study of self-masking nanostructuring of boron doped diamond films by RF plasma etching", Vacuum, vol. 169, p. 108954, 2019.

[11] O. Kádár, F. Uherek, J. Chlpík, J. Remsa, J. Bruncko, A. Vincze, „Characterization and optical properties of TiO_2 prepared by pulsed laser deposition", in 2010 International Conference on Applied Electronics, pp. 141–144, 2010.

[12] T. Klein, P. Achatz, J. Kacmarcik, C. Marcenat, F. Gustafsson, J. Marcus, E. Bustarret, J. Pernot, F. Omnes et al., „Metal-insulator transition and superconductivity in boron-doped diamond", Physical Review B, vol. 75, no. 16, p. 165313, 2007.

[13] C. Terashima, R. Hishinuma, N. Roy, Y. Sugiyama, S. S. Latthe, K. Nakata, T. Kondo, M. Yuasa, A. Fujishima, "Charge Separation in TiO_2/BDD Heterojunction Thin Film for Enhanced Photoelectrochemical Performance", ACS Applied Materials & Interfaces, vol. 8, no. 3, pp. 1583–1588, 2016.

[14] J. Ćirković, A. Radojković, D. Luković Golić, N. Tasić, M. Čizmić, G. Branković, Z. Branković, "Visible-light photocatalytic degradation of Mordant Blue 9 by single-phase BiFeO3 nanoparticles", Journal of Environmental Chemical Engineering, vol. 9, no. 1, p. 104587, 2021.

[15] M. N. Pervez, F. Y. Telegin, Y. Cai, D. Xia, T. Zarra, V. Naddeo, "Efficient Degradation of Mordant Blue 9 Using the Fenton-Activated Persulfate System", Water, vol. 11, no. 12, p. 2532, 2019.

[16] C. A. Martínez-Huitle, M. A. Rodrigo, I. Sirés, O. Scialdone, "Single and coupled electrochemical processes and reactors for the abatement of organic water pollutants: A critical review", Chemical Reviews, vol. 115, no. 24, pp. 13362–13407, 2015.

[17] G. C. Tedesco, C. A. Joll, W. P. Ela, A. Pivrikas, D. J. Henry, „3D-Printed TiO_2 Electrode as a Viable Alternative for Photoelectrocatalytic Purification of Water", ChemistrySelect, vol. 8, no. 38, p. e202300288, 2023.

[18] P. A. Carneiro, M. E. Osugi, J. J. Sene, M. A. Anderson, M. V. B. Zanoni, „Evaluation of color removal and degradation of a reactive textile azo dye on nanoporous TiO_2 thin-film electrodes“, Electrochimica Acta, vol. 49, no. 22–23, pp. 3807–3820, 2004.

[19] J. R. Huang, X. Tan, T. Yu, L. Zhao, W.-L. Hu, „Enhanced Photoelectrocatalytic and Photoelectrochemical Properties by High-Reactive TiO_2/$SrTiO_3$ Hetero-Structured Nanotubes with dominant {001} Facet of Anatase TiO_2“, Electrochimica Acta, vol. 146, pp. 320–328, 2014.

Received 2 June 2026